XVII[èmes] *Journées Nationales Génie Côtier – Génie Civil*
Chatou, 2022
DOI:10.5150/jngcgc.2022.007 *© Editions Paralia CFL*
disponible en ligne – http://www.paralia.fr – available online

Hydrodynamic simulations of flow around a wall-mounted cylinder using RANS, LES and hybrid RANS-LES turbulence models

Alban GILLETTA DE SAINT JOSEPH [1], Julien CHAUCHAT [2], Cyrille BONAMY [2], Marie ROBERT [1]

1. France Énergies Marines, 525 avenue Alexis de Rochon, 29280 Plouzané, France.
   alban.gilletta@france-energies-marines.org; marie.robert@france-energies-marines.org
2. Université de Grenoble Alpes, LEGI, UMR 5519 CNRS, Domaine Universitaire, CS 40700, 38058 Grenoble, France.
   julien.chauchat@univ-grenoble-alpes.fr; cyrille.bonamy@univ-grenoble-alpes.fr

Abstract:
In the context of Offshore Wind Farms (OWF), hydrodynamic and turbulence play a major role in scour phenomenon. Nowadays, many simulations are performed using Reynolds-Averaged Navier-Stokes (RANS) turbulence models that enable fast, stable and coherent calculation but suffer from a lack of accuracy. The increasing use of turbulence resolving simulations such as Large Eddy Simulation (LES) or more recently hybrid RANS-LES has led to significant progress in fluid mechanics and engineering. In order to objectively evaluate the various existing turbulence models a simpler configuration than an obstacle facing steady current, namely the plane channel flow, is used in the first part of the present work. The knowledge gained on the plane channel flow case is then used to evaluate the different turbulence modelling approaches for an obstacle facing steady current in the context of offshore wind farm field. This part focuses on a circular pile facing steady current using RANS, LES and hybrid RANS-LES. All the simulations presented in this work have been performed using OpenFOAM an open-source Computational Fluid Dynamics (CFD) toolbox.

Keywords:
Offshore Wind Farms, Scour, Turbulence modelling, Large Eddy Simulation (LES).

1. Introduction

Offshore Wind Energy has benefited from a strong impulse during the last decade in France aiming at complementing the national energetic mix plan. Implementation of such infrastructure is challenging due to maritime hydraulic and sediment transport that occur at high level especially in the English Channel where future OWF are planned. MODULLES French project led by France Énergies Marines looks into the interactions between mobile submarine dunes and OWF off Dunkirk. This work focuses on the small scale hydrodynamic in the vicinity of the pile where scour phenomenon takes place. Scouring process is mainly driven by the turbulent eddies generated by the presence of the structure, namely the horseshoe vortex (HSV) system upstream and the vortex shedding downstream. The ability to reproduce these vortices strongly depends on the accuracy of the turbulence model. Many numerical studies have been carried out using different turbulence approaches such as Reynolds-Average Navier-Stokes (RANS), Large Eddy Simulation (LES) and hybrid RANS-LES. For a steady current around a cylinder, the three turbulence modelling approaches have been compared with experimental data (ROULUND *et al.*, 2005). Unsteady RANS (URANS) simulations allow reproducing the mean flow field reasonably well at an affordable computational cost, still it cannot reproduce accurately the vortex dynamic around the structure (NAGEL *et al.*, 2020). The idea behind hybrid RANS-LES and LES approaches is to resolve large eddies structures that carry most of the energy. In these later approaches, one of the key issues is to impose a realistic turbulence at the inlet (KIRKIL & CONSTANTINESCU, 2015). Another important parameter is near wall refinement used when dealing with turbulence approach, as it directly affects the boundary layer modelling. Numerical schemes also play a major role on the results for the calculation stability and accuracy. Simulations have been performed using the solver pimpleFOAM with Improved Delayed Detached-Eddy Simulation called IDDES in this work (GRITSKEVICH *et al.*, 2012), Smagorinsky (SMAGORINSKY, 1963) and dynamic Lagrangian (MENEVEAU *et al.*, 1996) models available in OpenFOAM (JASAK & Uroić, 2020). In this contribution, different combinations of turbulence models, numerical schemes, mesh refinement, inlet turbulence have been performed on plane channel configuration as a first step before test on the wall-mounted cylinder case.

2. Models, equations and configurations

2.1 Navier-Stokes equations

OpenFOAM uses Finite Volume Discretization of Navier-Stokes (NS) equations for incompressible and unsteady flow with pimpleFOAM solver. The general formulation of NS equations including turbulent viscosity assumptions is presented by the coupled mass conservation equation (1) and momentum equation (2).

$$\nabla . \vec{U} = 0 \quad (1)$$

$$\frac{d\vec{U}}{dt} + \nabla.\left(\vec{U} \otimes \vec{U}\right) = \frac{-\nabla p}{\rho} + \nabla.\left[\left(\nu + \nu_t\right)\left(\nabla\vec{U} + \nabla\vec{U}^t\right)\right] \quad (2)$$

where : $\vec{U}$ is the velocity vector, p is the pressure, ν is the kinematic viscosity, ν_t is the turbulent kinematic viscosity and ρ is the density of the fluid.

2.2 Turbulence model

In order to model turbulence, a time-averaging operator is applied to the NS equations for RANS while a filtering operator is used for LES. The application of the operator brings up higher-order correlations that need to be modelled using a turbulent eddy viscosity or subgrid-scale viscosity. In this work, the following turbulence models are considered: RANS k-ω SST (3), LES Smagorinsky (4), LES dynamic Lagrangian (5) and hybrid IDDES.

$$\nu_{t_{RANS}} = a_1 \frac{k}{\max(a_1\omega, \Omega F_2)} \quad (3)$$

where a_1 is a constant, k is the Turbulent Kinetic Energy (TKE), ω is the turbulent specific dissipation rate, Ω is the vorticity magnitude and F_2 is a blending function.

Note that two transport equations, one for k and one for ω, need to be solved in this model to close the system. The k-ω SST model behaves as a standard k-ω model in the viscous sublayer and as a k-ε model in the outer layer.

For LES models, the subgrid-scale viscosity may be written as:

$$\nu_{t_{LES}} = (C_S\Delta)^2|\bar{S}| \quad (4)$$

where C_S is the Smagorinsky constant, Δ is the integral scale of the subgrid-scale and $|\bar{S}|$ is the second invariant of the filtered field deformation tensor, quantifying the characteristic velocity of subgrid eddies.

Note that for the dynamic Lagrangian formulation C_S is no longer a constant and varies spatially and over time:

$$C_S^2 = C(\vec{x}, t) \quad (5)$$

The Dynamic Lagrangian model is included in the dynamic Smagorinsky approach and based on the idea of double filtering NS equations showing an additional tensor that represents the resolved turbulent stresses between the width of the two filters.

Hybrid IDDES turbulence approach is a mix between LES and RANS k-ω SST model. Switch between the two approaches depends not only on grid size but also on the wall-distance.

2.3 Turbulence inlet

Having a well-developed turbulent flow at the inlet for a LES or a hybrid simulation is important to reproduce the upstream flow field with potential important impact on the dynamic of the HSV system. In the present contribution, different approaches are tested, Divergence Free Synthetic Eddy Method (DFSEM, POLETTO *et al.*, 2013) and periodic boundary condition with initial perturbation. DFSEM generates synthetic eddies based on random locations and intensities, with as input parameters Reynolds stress components,

correlation length of turbulence structure and a bulk velocity with a divergence free property.

2.4 Cases descriptions

Two configurations are studied in the present article. First, the plane channel flow configuration which has been extensively studied to evaluate turbulence approaches, turbulence inlet condition precedingly introduced and mesh refinement (see Table 1). For LES dynamic Lagrangian model, numerical temporal and spatial discretization schemes are second order with a high-frequency filter, denoted as filter in the following. The computational domain is 6D long, 3D wide and 1D high with D equal to 0.536 m. D refers to cylinder diameter in ROULUND *et al.*, (2005) experiment. The depth-averaged velocity is 0.326 m/s leading to a Reynolds number of about 1.7 10^5. Periodic boundary conditions are used on sides of the computational domain, slip condition at the top boundary while a no slip condition is used at the smooth bottom boundary.

The wall-mounted cylinder configuration is similar to ROULUND *et al.*, 2005 experiment, the incoming flow is steady and unidirectional over a rigid-bed. The computational domain is 12D long, 8D wide and 1D high. Periodic boundary conditions cannot be used in the presence of the cylinder and an alternative solution has to be implemented. Mapped patch boundary condition fixes an offset length where the flow is periodic in which the turbulence can develop without increasing too much the computational domain length. A numerical simulation using mapped inlet boundary condition has been performed but it was unsuccessful, the velocity slowed down in the central zone in front of the cylinder and accelerated on the sides due to the obstacle presence. Consequently, despite results from plane channel case, DFSEM seems to be more appropriate for the inlet boundary condition for hybrid and LES simulations of the flow around a wall-mounted cylinder. Both configurations are shown in figure 1.

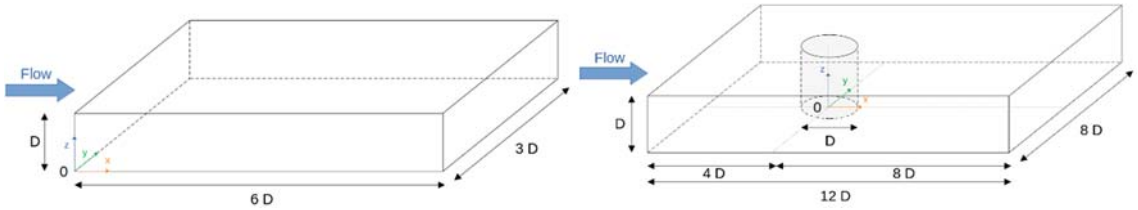

Figure 1. Sketch of the plane channel flow (left) and wall-mounted cylinder configurations (right).

3. Results

3.1 Plane channel case

Figure 2 represents three vertical profiles of the velocity, Reynolds stress and TKE scaled with friction velocity u_*=0.013 m/s (from experiments) and plotted over wall units. Three

different meshes (see table 1) are tested for LES dynamic Lagrangian model, with streamwise periodic boundary conditions and a filter scheme. Our results show reasonable agreement for the velocity profile with mesh M3 (green line) indicating that a fine mesh is required for this problem. Indeed, as the refinement increases, more turbulent structures are resolved, leading to a larger value for Reynolds stress. For LES, the first grid point should be about 1 wall unit in the vertical direction, 22.5 and 90 wall units respectively in the spanwise and streamwise directions according to lectures notes of MÉTAIS, 2018. TKE peak is decreased with the refinement and shifted at lower elevation. It is still high but closer to FUHRMAN *et al.*, (2010) who directly measured fluctuating velocity components in a steady, uniform, open-channel flow at a Reynolds number of 1.9 10^4.

Table 1. Mesh refinement for plane channel case.

Mesh name	***Mesh refinement (wall unit = Δu*/ν)***		***Number of cells***
	spanwise/streamwise	***vertical***	
M1	*250*	*4*	*1.8 10^6*
M2	*160*	*4*	*4.3 10^6*
M3	*100*	*2*	*1.7 10^7*

where Δ is the cell size.

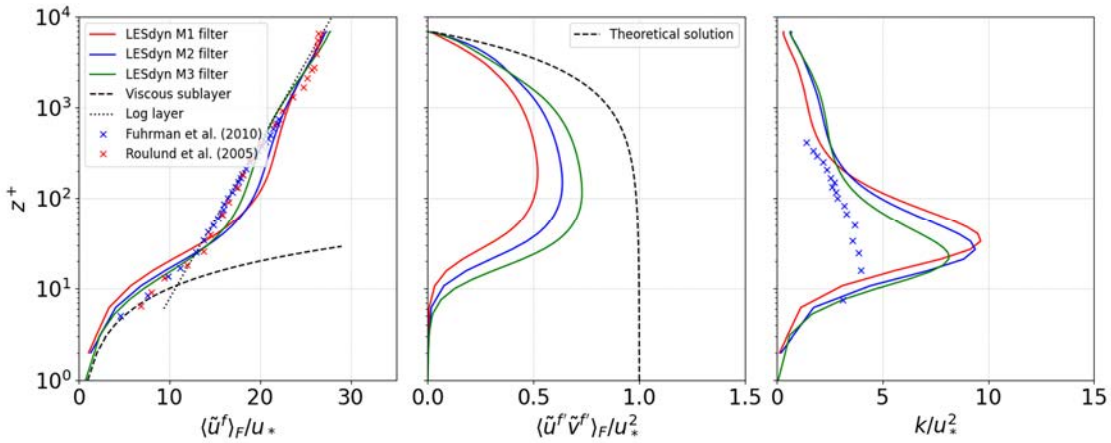

Figure 2. Dimensionless time and space averaged over the whole domain velocity profile (left), Reynolds stress x-y component (centre) and TKE (right) with different meshes M1, M2 and M3.

Figure 3 presents IDDES M1 solution (red line), showing improved agreement with theoretical and experimental results for the velocity profile compared with LES dynamic Lagrangian results (blue line). Concerning Reynolds stress, the IDDES results are closer to the theory meaning that large structures are quite well resolved away from the bottom as the IDDES turns in LES mode. TKE profile predicted by the IDDES model are in better agreement with FUHRMAN *et al.*, 2010. The velocity profile predicted by the LES model

shows discrepancies but follows more or less the expected shape. This test clearly demonstrates that, for such high Reynolds number, the hybrid RANS-LES (IDDES) model is promising, especially when using a rather coarse mesh compared with LES requirements. This result is very important for simulations around an obstacle as the number of grid points will increase dramatically.

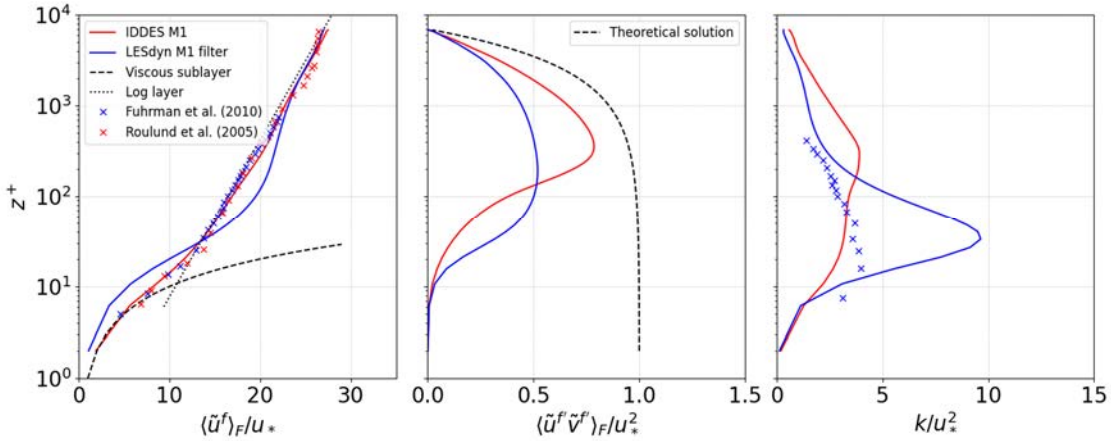

Figure 3. Dimensionless time and space averaged over the whole domain velocity profile (left), Reynolds stress x-y component (centre) and TKE (right) with periodic boundary conditions with initial perturbation.

The final objective is to impose a realistic turbulent boundary condition at the inlet for the wall-mounted cylinder case for which periodic boundary conditions cannot be used. Consequently, different approaches for the inlet have been tested as shown in figure 4. It illustrates the profiles for the same simulations as in figure 3 but with DFSEM turbulence inlet condition. The results obtained with IDDES M1 (red line) reproduces relatively well the viscous sublayer velocity profile but it slightly underestimates the buffer layer and overestimates the second part of the log layer. The fact that the Reynolds shear stress and TKE profiles are underestimated clearly shows that the boundary layer is not fully developed. The same conclusions can be made on the LES simulation results (blue line) with even larger discrepancies. The comparison between periodic boundary condition simulations and DFSEM simulations allows us to clearly identify the weaknesses of DFSEM. In the present case, the computational domain length is too short with DFSEM to represent a fully developed turbulent flow. The problem is more pronounced with LES than IDDES.

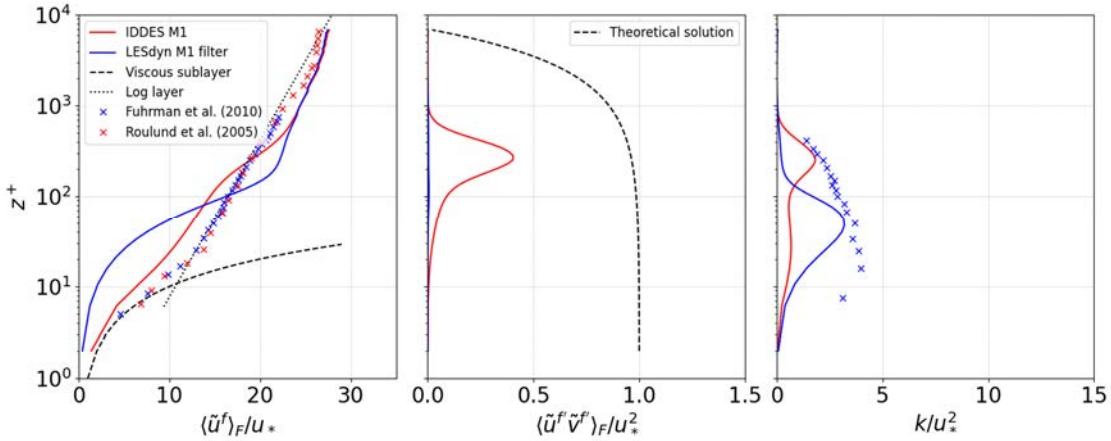

Figure 4. Dimensionless time and space averaged over the domain between x = 4.5D to x = 5.25D velocity profile (left), Reynolds stress x-y component (centre) and TKE (right) with DFSEM turbulence inlet condition.

3.2 Wall-mounted cylinder case

Figure 5 shows time-averaged streamwise and vertical velocity profiles at different elevations for three simulations using hybrid RANS-LES (IDDES) model and LES (Smagorinsky and dynamic Lagrangian) models. Note that the three configurations use DFSEM boundary condition at the inlet second order central differencing scheme and medium mesh M2. It can be inferred that the Smagorinsky model (green line) does not predict correctly the HSV region compared with experiments (red dots) from ROULUND *et al.*, 2005 while it is in good agreement for the dynamic Lagrangian model (purple line) and IDDES (blue line) models. The LES Smagorinsky model is not suitable in the wall-mounted cylinder case and consequently should be avoided.

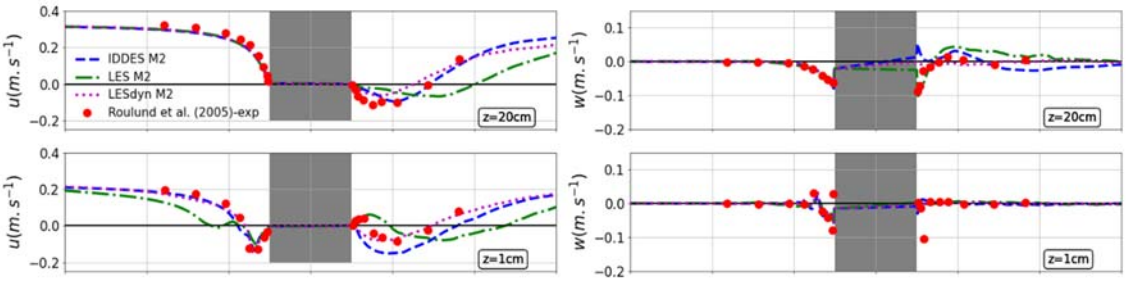

Figure 5. Time-averaged velocity profile of streamwise (left) and vertical (right) component in the symmetry plane at different elevations

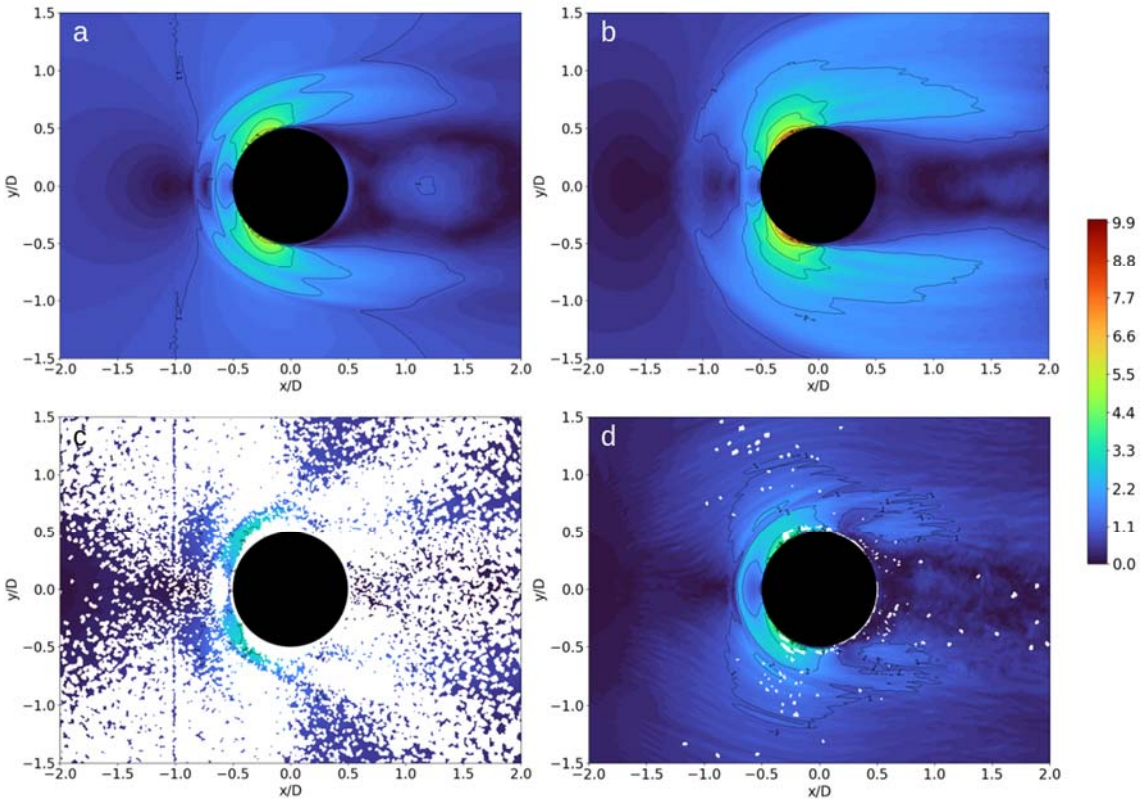

Figure 6. Averaged bottom shear stress amplification $|\tau_0 / \tau_\infty|$ with IDDES (a), Smagorinsky (b) and dynamic Lagrangian model with linear (c) and filter scheme (d).

Figure 6 shows averaged bottom shear stress amplification map for four simulations. While IDDES and Smagorinsky models remain stable and coherent, dynamic Lagrangian model results show strong numerical instabilities. It might be due to the use of second order central differencing scheme (figure 6c), more accurate but too unstable to be used with dynamic Lagrangian model. Figure 6d uses filter scheme, similar to Total Variation Diminishing (TVD) schemes, and exhibits more acceptable results even if few instabilities are still remaining. Note that this result is extracted from not fully converged simulation.

4. Conclusions

Simulations in plane channel case emphasized DFSEM limits when dealing with small computational domain length and periodic boundary condition should be used in the first place. IDDES simulations show promising results at coarse mesh refinement while LES is getting accurate only with a fine mesh which can lead to important computational cost. Despite other tests and previous results, wall-mounted cylinder simulations were performed with DFSEM using hybrid and LES turbulence approaches. The comparison proves the superiority of dynamic Lagrangian model to reproduce the mean velocity field while IDDES shows promising result at coarse mesh. IDDES and Smagorinsky attest

stable and coherent features in the bottom shear stress variable unlike dynamic Lagrangian that requires TVD schemes to reduce numerical instabilities. In the perspective of assessing scour through sediment transport modelling, bottom shear stress is a key variable and needs to be accurately solved. The results presented here will be used as guidelines for the next stage of the work.

5. References

FUHRMAN D. R., DIXEN M., JACOBSEN N. G. (2010). *Physically-consistent wall boundary conditions for the k-ω turbulence model*. Journal of Hydraulic Research, Vol. 48, pp. 793-800. http://dx.doi.org/10.1080/00221686.531100

GRITSKEVICH M. S., GARBARUK A. V., SCHÜTZE J., MENTER F.R. (2012). *Development of DDES and IDDES Formulations for the k-ω SST Model*. Flow Turbulence Combust, Vol. 88, pp. 431-449. https://doi.org/10.1007/s10494-011-9378-4

JASAK H., UROIĆ T. (2020). *Practical computational fluid dynamics with the finite volume method. In Modeling in Engineering Using Innovative Numerical Methods for Solids and Fluids*, pp. 103-161. Springer.

KIRKIL G., CONSTANTINESCU G. (2015). *Effects of cylinder Reynolds number on the turbulent horseshoe vortex system and near wake of a surface-mounted circular cylinder*. Physics of Fluids, Vol. 27, pp. 075-102. https://doi.org/10.1063/1.4923063MENEVEAU C., LUND T., CABOT W. (1996). *A Lagrangian dynamic subgrid-scale model of turbulence*. Journal of Fluid Mechanics, Vol. 319, pp. 353-385. https://doi.org/10.1017/S0022112096007379

MÉTAIS O. (2018). *Large Eddy Simulation of Turbulence : Fundamentals and Applications*. Lectures notes.

NAGEL T., CHAUCHAT J., BONAMY C., LIU X., CHENG Z., HSU T.-J. (2020). *Three-dimensional scour simulations with two-phase flow model*. Advances in Water Ressources, Elsevier, Vol. 138, pp. 103544. https://doi.org/10.1016/j.advwatres.2020.103544

POLETTO R., CRAFT T., REVELL A. (2013). *A New Divergence Free Synthetic Eddy Method of the Reproduction of Inlet Flow Condition for LES*. Flow Turbulence and Combustion, Vol. 91, pp. 519-539. https://doi.org/10.1007/s10494-013-9488-2

SMAGORINSKY J. (1963). *General circulation experiments with the primitive equations*. Monthly Weather Review, Vol. 91, pp. 99-164. https://doi.org/10.1175/1520-0493(1963)091<0099:GCEWTP>2.3CO;2